Journal of Biomechanical Science and Engineering

Vol. 5, No. 5, 2010

Nasal Flow Simulation Using Heat and Humidity Models*

Kiyoshi KUMAHATA**, Futoshi MORI**, Shigeru ISHIKAWA***
and Teruo MATSUZAWA**

**Japan Advanced Institute of Science and Technology,
1-1 Asahidai, Nomi 923-1292, Ishikawa, Japan
E-mail: {k_kuma, f-mori, matuzawa}@jaist.ac.jp
***Kanazawa Municipal Hospital,
3-7-3 Heiwamachi, Kanazawa 921-8105, Ishikawa, Japan

Abstract

The nasal cavity performs several important functions for the inhaled air, such as temperature and humidity adjustments. Although it is necessary to obtain velocity, temperature, and humidity distributions during inhalation in order to understand the nasal cavity's functions, it is difficult to measure them noninvasively in the nasal cavity. Therefore, we have continued to study nasal flow simulation with heat and humidity transport. In such a simulation, the governing equations include a continuum equation and the equations describing momentum, energy, and water transport. The temperature and humidity of the inhaled air are adjusted by heat and water exchange on the nasal cavity wall's surface. Therefore, in the simulation, these roles of the wall in the energy and water transport equations were included as the boundary conditions. Although in related studies of nasal flow simulation with heat and humidity transport, the nasal cavity wall's surface temperature and humidity were constant, here they were treated as degrees of using Newton's cooling law. A flow including temperature and humidity in a realistic human nasal cavity shape was simulated. The simulation results agreed well with the measurements reported by Keck at al. Therefore, this study concludes that our model can simulate the heat and humidity exchange occurring in the nasal cavity. In addition, it was found that the temperature and humidity adjustment functions worked effectively in the front and narrow regions of the nasal cavity.

Key words: Nasal Flow, Computational Fluid Dynamics, Realistic Shape, Heat and Humidity

1. Introduction

The nasal cavity performs several important functions for the inhaled air, such as temperature and humidity adjustments, filtering, and smell sensing. The temperature adjustment function heats or cools the inhaled air when the outer air is cooler or warmer than the body temperature, respectively. The humidity adjustment function humidifies or dries the inhaled air when the outer air is dryer or wetter than the body, respectively. The filtering function removes dust from the inhaled air. The smell-sensing function works by transporting odor molecules into the olfactory cleft, which is a region of the nasal cavity that senses smells. The temperature and humidity adjustment functions are biologically important because the differences in these temperature and humidity adjustment functions between humans and apes cause a difference in adaptability to the living environment[(1)]. Although the flow must be measured during inhalation in order to understand the nasal

*Received 14 June, 2010 (No. 10-0251)
[DOI: 10.1299/jbse.5.565]

cavity's functions, it is difficult to measure noninvasively in the nasal cavity. Therefore, computational fluid dynamics (CFD) approaches are useful. Wen et al.[2] investigated the three-dimensional flow velocity field and the flow rate distribution of a geometrical region in the nasal cavity by the finite volume method. Finck et al.[3] studied the velocity and pressure distributions during inhalation and exhalation by the lattice Boltzmann method. Lee et al.[4] simulated the velocity, pressure, and temperature distribution using time-dependent outlet pressure and wall temperature for a breath cycle.

This paper demonstrates nasal flow simulation with heat and humidity transport in order to understand how the nasal cavity adjusts the temperature and humidity of the inhaled air. In this simulation, the governing equations include the continuum equation, which describes mass conservation; the Navier–Stokes equation, which describes momentum transport; the energy equation, which describes energy transport; and the water transport equation. The temperature and humidity of the inhaled air are adjusted by exchanging heat and water between the organ side and the air side via the mucous membrane covering the nasal cavity wall. Therefore, for numerical fluid simulation with heat and humidity transport, models of these roles of the wall were constructed and implemented as the boundary conditions for solving the energy and water transport equations. For the temperature boundary condition in the energy equation, the wall surface temperature was treated as a degree of freedom determined by the temperature difference between air and the organ via the membrane by using Newton's cooling law. The humidity boundary condition for the water transport equation was also implemented by the same mechanism, in which water moves between air and the organ via the membrane. By using these temperature and humidity adjustment models, nasal flow with temperature and humidity transport in a realistic human nasal cavity shape reconstructed from computed tomography (CT) images was simulated. The simulation results agreed well with the measurements reported by Keck et al.[5]. In addition, two cases of inhaled air temperature and humidity were simulated. The temperature and humidity were found to be effectively and efficiently adjusted in the front region of the nasal cavity during inhalation. The following sections describe the flow model, heat and water exchange models, verification, and numerical experiments.

2. Model of Flow in Nasal Cavity

This study modeled an incompressible, viscid, laminar air flow in the nasal cavity with heat and humidity transport. Turbulence was not modeled because the maximum Reynolds number of the inhaled flow was lower than the critical Reynolds number. Here, humidity generally implies relative humidity and is the ratio of the amount of water contained in air to the saturation capacity of air. However, the saturation capacity changes with temperature. Hence, it is difficult to directly treat relative humidity as a degree of freedom. Therefore, to model the magnitude of humidity in air, we considered the concentration of water in air instead of treating the relative humidity directly. Although various approaches have been used to represent the concentration of water, the mass fraction of water, that is, the ratio of the weight of water to the weight of humid air was employed as a degree of freedom. Thus, for nasal flow with heat and humidity transport, the phenomena that should be considered include fluid flow, heat transport, and water transport. The degrees of freedom included four variables: velocity, pressure, temperature, and mass fraction of water. Accordingly, the governing equations were as follows: equation of momentum, Eq. (1); equation of conservation of mass, Eq. (2); transport equation of energy, Eq. (3); and transport equation of the mass fraction of water, Eq. (4).

$$\rho\left\{\frac{\partial \boldsymbol{u}}{\partial t}+(\boldsymbol{u}\cdot\nabla)\boldsymbol{u}\right\}=-\nabla p+\mu\nabla^2\boldsymbol{u} \tag{1}$$

$$\nabla\cdot\boldsymbol{u}=0 \tag{2}$$

$$\rho Cp\left\{\frac{\partial T}{\partial t}+(\boldsymbol{u}\cdot\nabla)T\right\}=K\nabla^2T \tag{3}$$

$$\frac{\partial F}{\partial t}+(\boldsymbol{u}\cdot\nabla)F=D\nabla^2F \tag{4}$$

Here, t, $\boldsymbol{u}$, p, ρ, ν, K, T, Cp, F, and D denote time, velocity, pressure, density, kinematic viscosity, thermal conductivity, temperature, specific heat, mass fraction of water, and mass diffusion coefficient, respectively. To solve this equation system comprising Eqs. (1) to (4), the general purpose fluid simulation software FLUENT[6] by ANSYS, Inc. was employed. To incorporate the temperature and humidity adjustment functions of the nasal cavity, it is necessary to introduce appropriate boundary conditions that represent the heat and water exchange occurring on the nasal cavity wall in order to solve the transport equations of energy and mass fraction of water.

3. Boundary Conditions for Energy and Transport Equations

The nasal cavity wall has a layered structure consisting of a mucous membrane and a capillary layer consisting of capillaries located on the organ side, as shown in Fig. 1. The temperature and humidity of the inhaled air are adjusted by heat and water exchanges between the organ side and the air side via the mucous membrane. Zachow et al.[7] showed the temperature and humidity distribution in the nasal cavity during a breath under a boundary condition of constant temperature and humidity on the nasal cavity wall surface. Naftali et al.[8] calculated the nasal flow with temperature and humidity transport. However, these studies were conducted without considering the mucous membrane thickness and the effect of temperature and humidity changes on the mucous membrane due to the inhaled air. To consider these effects as the boundary conditions for the energy equation Eq. (3) and the transport equation Eq. (4), heat and water exchanges via a thin mucous membrane were modeled in this study; the model includes the mucous membrane thickness. It can consider the effect of the inhaled air on the temperature and humidity of the nasal cavity wall surface by treating the temperature and humidity of this surface as a degree of freedom. This model represents the air side region as a computational mesh reconstructed from the binarization of a CT image using air brightness in the image. The organ-side region is treated as not a computational mesh but a mathematical model that covers the air side region.

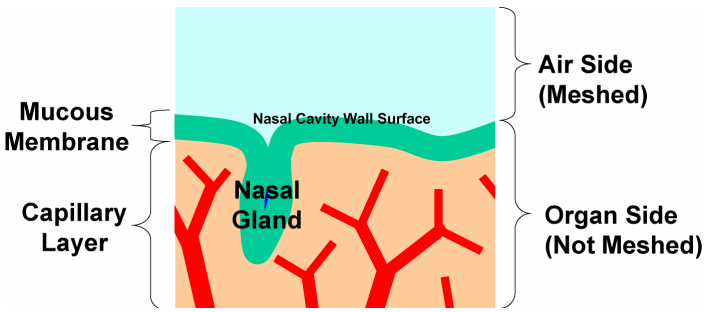

Fig. 1 Structure of Nasal Cavity Wall:
Nasal cavity wall surface is covered with mucous membrane. Mucous membrane has a nasal gland that secretes mucus. Cilia and nose hairs are ignored in this figure. Capillaries supply materials for mucus.

3.1 Model of Heat Exchange on Cavity Wall for a Boundary Condition of the Energy Equation

Figure 2 illustrates the exchange of heat between the organ side and the air side via the mucous membrane. In this figure, δ_{memb} represents the membrane's thickness. This membrane is a simplified model of the actual mucous membrane, which ignores nasal glands and small objects on the membrane's surface, such as cilia and nose hairs. The nasal cavity, i.e., the air region, is represented by a computational mesh. The membrane and the organ side region are represented by a mathematical model attached to the outside of the nasal-cavity-shaped mesh. T_O indicates the temperature of the organ side; it is a constant value because the organ side is provided with sufficient heat by the capillary layer. T_S denotes the temperature of the membrane surface, which is not constant but rather a degree of freedom that should be determined by calculation. Q_{memb}, indicated by a red arrow, represents the heat flux transmitted between the organ side and the air side via the membrane. Q_{memb} is defined by Eq. (5).

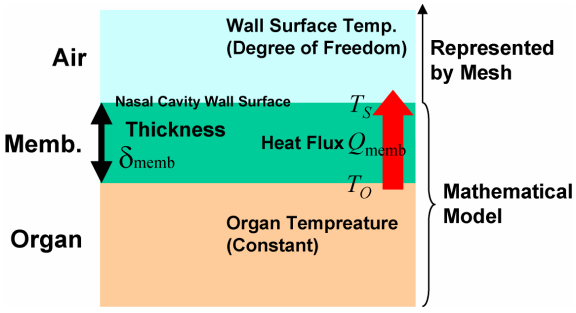

Fig. 2 Model for Heat Exchange on Nasal Cavity Wall:
Heat is transmitted between the organ side and the air side via the membrane. T_O, T_S, Q_{memb}, and δ_{memb} represent the nasal cavity wall surface temperature, organ side temperature, heat flux, and membrane thickness, respectively. T_O is treated as a constant and T_S is a degree of freedom that must be calculated.

$$Q_{memb} = K_{memb}\frac{\partial T}{\partial \boldsymbol{n}} = K_{memb}\frac{T_O - T_S}{\delta_{memb}} \tag{5}$$

K_{memb} and $\boldsymbol{n}$ denote the thermal conductivity of the membrane and the normal vector of the nasal cavity wall surface, respectively. If $T_O > T_S$, Q_{memb} is transmitted into the air side from the organ side, and the inhaled air is heated as heat flows into it from the organ side. If $T_O < T_S$, Q_{memb} is transmitted into the organ side from the air side, and the inhaled air is cooled as heat is transferred from it to the organ side. Heat transfer between the organ side and the air side is included in the nasal flow simulation by using the heat flux Q_{memb} defined by Eq. (5) as a flux boundary condition for the energy equation Eq. (3). It was implemented in a CFD procedure using the heat transfer boundary condition that is normally provided as a FLUENT function.

3.2 Model of Water Exchange on Cavity Wall for a Boundary Condition of the Transport Equation

Figure 3 illustrates the exchange of water between the organ side and the air side via the mucous membrane. δ_{memb} denotes the membrane's thickness. This membrane is a simplified model of the actual mucous membrane and is the same as that used to construct the heat exchange model. F_O indicates the mass fraction of water on the organ side and is a constant value because the organ side is provided with sufficient water by the capillary layer. F_S denotes the mass fraction of water on the membrane's surface, which is not a constant but rather a degree of freedom that should be determined by calculation. W_{memb}, indicated by a blue arrow, represents the water flux transmitted between the organ side and the air side via

the membrane. W_{memb} is defined by Eq. (6).

$$W_{memb} = D_{\text{memb}} \frac{\partial F}{\partial \boldsymbol{n}} = D_{\text{memb}} \frac{F_O - F_S}{\delta_{\text{memb}}} \tag{6}$$

D_{memb} and $\boldsymbol{n}$ represent the mass diffusion coefficient of the membrane and the normal vector of the nasal cavity wall surface, respectively. If $F_O > F_S$, W_{memb} is transmitted into the air side from the organ side, and the inhaled air is humidified as water flows into it from the organ side. If $F_O < F_S$, W_{memb} is transmitted into the organ side from the air side, and the inhaled air is dried as water is transferred from it to the organ side.

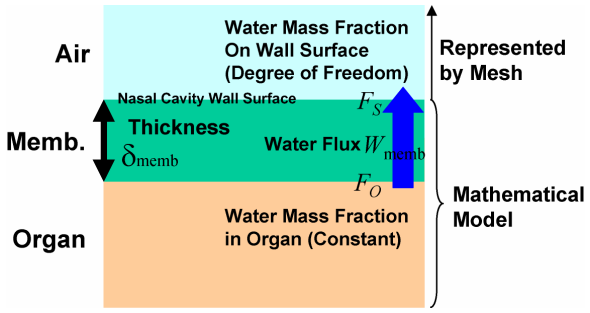

Fig. 3 Model for Water Exchange on Nasal Cavity Wall:
Water moves between the organ side and the airside via the membrane. F_S, F_O, W_{memb}, and δ_{memb} represent the mass fraction of water on the nasal cavity wall surface, the mass fraction of water on the organ side, the water flux, and the membrane thickness, respectively. F_O is treated as a constant and F_S is a degree of freedom that must be calculated.

Although FLUENT can easily deal with a boundary condition that specifies the heat flux at a boundary, it cannot deal with one that specifies the mass flux of the species transported through the boundary. For the species transport equation, FLUENT has only a Dirichlet-type boundary condition. It is necessary to determine the mass fraction of water on the nasal cavity wall surface. Therefore, a two-film theory was employed to determine this value. This theory is familiar in the chemical engineering field and is typically used to describe species transport between a liquid phase and a gas phase via a boundary. The theory assumes two thin layers on both sides of the boundary when a species is transported through the boundary. Because the species transported to the gas phase from the liquid phase pass through the liquid and gas side layers, the fluxes in both layers should be equal. The model for water exchange on the nasal cavity surface was modified using this theory.

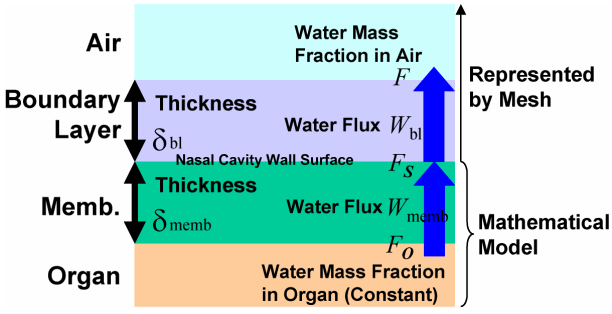

Fig. 4 Modified Water Exchange Model Using Two-Film Theory:
Water moves between the organ side and the air side via the membrane and the boundary layer. F, δ_{bl}, W_{memb}, and W_{bl} represent the mass fraction of water on the air side, the boundary layer thickness, the water flux in the membrane, and the water flux in the boundary layer, respectively.

Figure 4 shows the water exchange model modified by applying the two-film theory. The modification added an additional layer called the boundary layer next to the nasal cavity wall surface on the air side. In this figure, δ_{bl} denotes the boundary layer thickness. The air region and the boundary layer are represented by a computational mesh. The membrane and the organ side region are represented by a mathematical model attached to the outside of the nasal-cavity-shaped mesh. W_{memb} indicates the water flux between the organ side and the boundary layer via the membrane. W_{bl} represents the water flux between the membrane and the air side via the boundary layer. F signifies the mass fraction of water on the air side. The governing equations of the water fluxes W_{memb} and W_{bl} are Eqs. (7) and (8), respectively.

$$W_{\text{memb}} = D_{\text{memb}} \frac{\partial F}{\partial \boldsymbol{n}} = D_{\text{memb}} \frac{F_O - F_S}{\delta_{\text{memb}}} \tag{7}$$

$$W_{bl} = D_{\text{bl}} \frac{\partial F}{\partial \boldsymbol{n}} =_{\text{bl}} \frac{F_S - F}{\delta_{\text{bl}}} \tag{8}$$

D_{bl} signifies the mass diffusion coefficient of the boundary layer. Since water moves from the organ side to the air side via the membrane and the boundary layer, the water fluxes W_{memb} and W_{bl} should be equal according to the two-film theory. F_s was obtained as shown in Eq. (9) by solving Eqs. (7) and (8). As noted above, FLUENT cannot deal with a flux boundary condition for the species transport equation. However, instead of using a Dirichlet-type boundary condition in which the mass fraction of water on the nasal cavity wall surface is always constant, a variable boundary condition in which this value can change according to the inhaled air's properties can be used for the water transport equation Eq. (4) by using this mode. This calculation was implemented in the solving procedure by using a user-defined function in FLUENT.

$$F_S = \frac{\left(\frac{D_{\text{memb}}}{\delta_{\text{memb}}}\right) F_O + \left(\frac{D_{\text{bl}}}{\delta_{\text{bl}}}\right) F}{\left(\frac{D_{\text{memb}}}{\delta_{\text{memb}}}\right) + \left(\frac{D_{\text{bl}}}{\delta_{bl}}\right)} \tag{9}$$

Figure 5 illustrates the essential procedure for solving the system of Eqs. (1) to (4) for the steady state using the heat and water models as the boundary conditions. First, the velocities u, v, w and the pressure p are calculated by the momentum equation Eq. (1) and the continuum equation Eq. (2). Second, to obtain the temperature T, the energy equation Eq. (3) is solved using the calculated velocity and the heat flux Q_{memb} defined by Eq. (5) as the boundary conditions. Third, the mass fraction of water F is computed by the transport equation Eq. (4) using the velocity and the mass fraction of water on the nasal cavity wall surface F_s defined by Eq. (9). Fourth, if the residuals of all variables, u, v, w, p, T, and F, drop below the convergence criterion defined when the solution procedure began, the procedure will stop.

4. Reconstruction of Nasal Cavity Shape

To simulate an actual nasal flow with heat and humidity transport by using the heat and water exchange models described above, an actual human nasal cavity shape was reconstructed from CT images. The nasal cavity shape used in this study was reconstructed from the slice images of a 31-year-old male who had never suffered from any disease related to the nasal cavity. The original CT images consisted of 100 sheets of the slice images, and each image had 512 × 512 pixels in the DICOM format. The image resolution

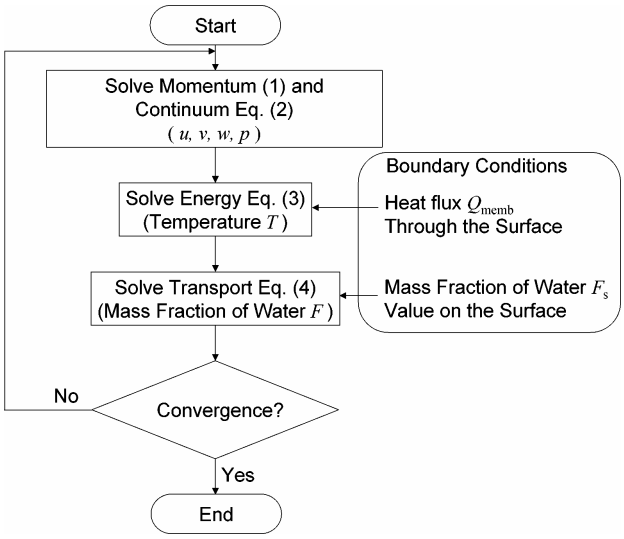

Fig. 5 Flowchart for Solving Nasal Flow with Temperature and Water Transport:
This figure shows the essential procedure for solving Eqs. (1) to (4) for the steady state.

was 0.186 mm/pixel in a slice image and 1.0 mm/slice between the slice images. Although the nasal cavity shape is generally asymmetric between the right and left sides and the shape changes with the nasal cycle, differences between the right and left sides of the nasal cavity were small. To reconstruct the nasal cavity shape as 3D polygon data, first, the paranasal sinuses, which are unnecessary for this study, were removed using the medical image processing software Real INTAGE[9]. Next, a 3D nasal cavity shape was constructed by reconstructing the 3D polygon data by using the marching cubes method[10][11]. Then, the polygons were optimized to remove warping by employing the polygon editing software Magics[12]. Finally, a computational mesh was obtained using the meshing tool in FLUENT. The mesh contained about 120×10^6 elements. The model's surface area and total volume were 149.95 cm^2 and 29.41 cm^3, respectively.

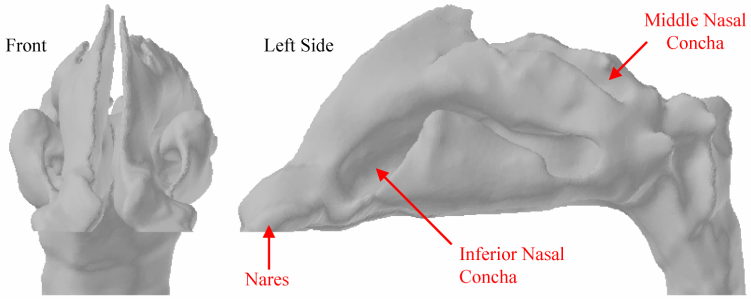

Fig. 6 Reconstructed Nasal Cavity Shape:
Shape was reconstructed from CT images of a 31-year-old male who had never suffered from any disease related to the nasal cavity. Nasal cavity is separated into three regions by two nasal conchae.

Figure 6 shows the reconstructed nasal cavity shape. The nasal cavity contains two large bulging areas, the middle nasal concha and the inferior nasal concha. Therefore, the nasal cavity is separated into three regions: the inferior meatus, middle meatus, and superior meatus. The inferior meatus is below the inferior nasal concha. The middle meatus is the region between the middle and inferior nasal conchae. The superior meatus is the region above the middle nasal concha.

5. Numerical Experiment

By using the heat and water exchange models and the reconstructed realistic nasal cavity shape, nasal flow with heat and humidity transport was simulated. First, the heat and water exchange models were verified and computational parameters were defined by comparing the simulation with the measurements. Next, to study the temperature and humidity adjustment functions of the nasal cavity, two cases of the inhaled air, the hot-wet case and the cold-dry case, were simulated.

5.1 Verification by Comparing the Simulation with Measurements

Keck et al. measured the temperature and humidity in the nasal cavity of 23 adults during inhalation by inserting a sensor. In Fig.7, red dots indicate the measurement points used by Keck et al. To verify the heat and water exchange models by comparing their results with the measurements, the simulated temperature and humidity were determined. The blue dots in Fig.7 indicate the evaluation points in the simulation.

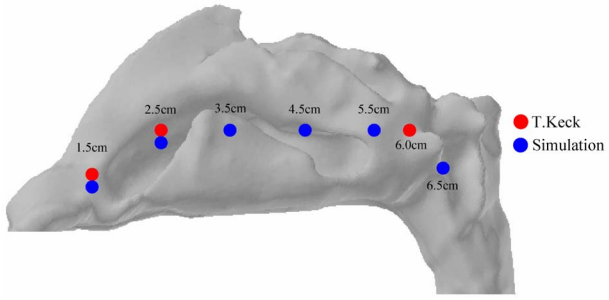

Fig. 7 Measurement Points:
Keck et al. measured the temperature and relative humidity in the nasal cavity of 23 adults during an inhalation; the measurements were performed at distances of 1.5, 2.5, and 6.0 cm from the nares by inserting a probe.

Simulations were performed under a steady state; that is, the calculated flow field was time-averaged field of an inhalation phase. For the boundary conditions of the numerical simulation, the nares were treated as free inlets. The temperature of the inhaled air was 25 °C and the mass fraction of water was 0.684%, for a relative humidity of 35% at 25 °C. The thermal conductivity and mass diffusion coefficient of the inhaled air were 0.0454 W/mK and 2.88×10^{-5} m^2/s, respectively. The pharynx was considered a velocity boundary that was assigned the velocity of the outflow from the nasal cavity. The steady velocity that means time-averaged velocity in an inhalation phase was 0.784 m/s. It was calculated using a pharynx cross-sectional area of 2.55 cm^2, a respiratory rate of 12 breaths/min, and a tidal volume 500.0 ml, which represents the tidal volume per breath. Under these conditions, the Reynolds number of the pharynx was 967 and the average Reynolds number of the nares was 465. The wall served as a non-slip boundary for the fluid velocity and incorporated the models for heat and water exchange.

As a parameter for the heat and water exchange models, ignoring the temperature dependence of the material parameters, the organ side temperature T_O was considered equal to the body temperature, 34 °C. The organ side mass fraction of water F_O was 3.34%, which is a relative humidity of 100% at 34 °C. The thermal conductivity of the membrane K_{memb} was 0.6 W/mK. The boundary layer thickness δ_{bl} was 1.0 mm. The mass diffusion coefficient of the membrane as a water vapor source D_{memb} was 2.6×10^{-5} m^2/s according to Lee et al.[13], assuming that the membrane was a high-density water vapor layer. Assuming that water vapor diffusion is stronger in the boundary layer than in the membrane, D_{bl} is 3.0

$\times 10^{-5}$ m^2/s. The membrane thickness δ_{memb} was 1.0, 2.0, 3.0, 4.0, or 5.0 mm. Figure 8 shows the boundary conditions and the material properties.

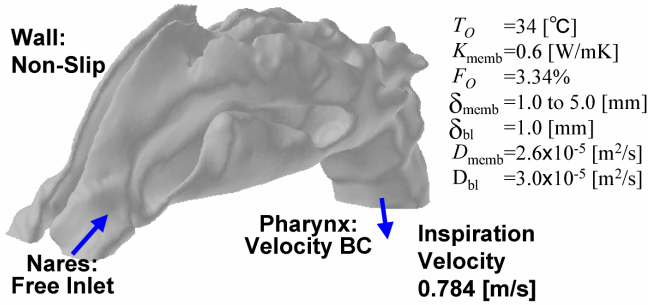

Fig. 8 Boundary Conditions for Simulation:
Pharynx was assigned an outward velocity of 0.784 m/s. Nares were treated as free inlets. Wall was a non-slip boundary. T_O, K_{memb}, F_O, δ_{memb}, and δ_{bl} indicate the organ-side temperature, thermal conductivity of the membrane, organ-side mass fraction of water (relative humidity of 100% at 34 °C), membrane thickness, and boundary layer thickness, respectively. D_{memb} indicates the mass diffusion coefficient of the membrane. D_{bl} represents the mass diffusion coefficient of the boundary layer in the double-film theory of the water exchange model.

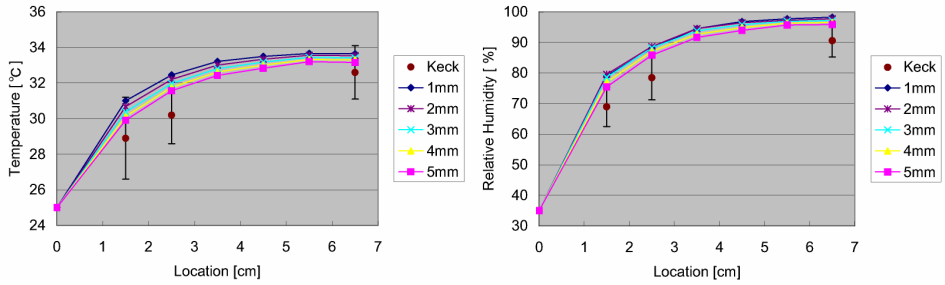

(a) Temperature (b) Relative Humidity

Fig. 9 Temperature and Relative Humidity Distribution:
Horizontal axis represents the location (distance from nares). Vertical axis represents temperature (a) and relative humidity (b). In the simulation results, the plotted temperature and relative humidity values are the spatial averages in each cross section located on the blue points in the Fig.7

Figure 9(a) shows the measured and simulated temperature distribution. The horizontal axis represents the location (distance from the nares) and the vertical axis represents temperature. For the results reported by Keck et al., the measured temperatures and error ranges were plotted. The temperature values of the simulated result on each location were the spatial averaged values in each cross section vertical to the direction from nares to pharynx, located on the blue points specified by Fig.7. In all cases, the measured and simulated values exhibited the same tendency: the temperature increased rapidly within 2.5 cm of the nares. Farther away, the temperature increased slowly, and the inhaled air was heated enough to approximate the body temperature, 34 °C. Furthermore, the tendencies observed for various δ_{memb} values were different; the rate of temperature increase decreased with an increase in δ_{memb}. This implies that a thicker membrane disturbed the heat transmission. For a thicker δ_{memb}, the simulation results were within the error range of the measurement. As mentioned above, the simulation results were the averaged temperature in the cross section at a specified location. Because the air temperature increased near the nasal cavity wall because of the high organ-side temperature of 34 °C, the averaged temperature was higher than the temperature of a point at the center of the flow. Considering this tendency of the averaged temperature, although the simulation results

seemed to be higher than the measured results at a first glance, they were in fact found to agree with the measured results.

Figure 9(b) shows the measured and simulated relative humidity distributions. The horizontal axis represents the distance of a point from the nares. The vertical axis represents the relative humidity. For the results reported by Keck et al., the measured relative humidity and error ranges were plotted. The relative humidity values of the simulated result on each location were the spatial averaged values in each cross section vertical to the direction from nares to pharynx, located on the blue points specified by Fig.7. In all cases, the measured and simulated values exhibited the same tendency: the relative humidity increased rapidly within 2.5 cm of the nares. Farther away, the relative humidity increased slowly and the inhaled air was sufficiently humidified to approximately 100%. In addition, the tendencies observed for various δ_{memb} values were different; the rate of relative humidity increase decreased with an increase in $\delta_{memb.}$ This implies that a thicker membrane disturbed water transport. Furthermore, for the thicker δ_{memb}, the simulation results were within the error range of the measurement. For the same reason as that mentioned earlier for temperature, the averaged relative humidity was higher than the relative humidity of a point at the center of the flow. Therefore, although the simulation results appeared to be higher than the measured results at first glance, they were in fact found to agree with the measurement results.

These results demonstrated that the heat and water exchange models could be used to simulate nasal flow with heat and humidity transport reasonably well. In the following subsection, we present simulation results for the cases of hot-wet and cold-dry inhaled air.

5.2 Simulation of Hot-Wet and Cold-Dry Inhaled Air

Here, to observe temperature adjustment and humidity adjustment functions of the nasal cavity, two cases of the inhaled air's properties were simulated. In case A, to observe these functions when the inhaled air was hot and wet, its temperature and relative humidity were set to 50 °C and 100%, respectively. In case B, to observe these functions when the inhaled air was cold and dry, its temperature and relative humidity were set to −10 °C and 10%, respectively. Thus, the mass fraction of water contained in the inhaled air was 7.95% for case A and 0.0175% for case B. Furthermore δ_{memb} was 3.0 mm. The other parameters were the same as those used in the abovementioned verification simulations.

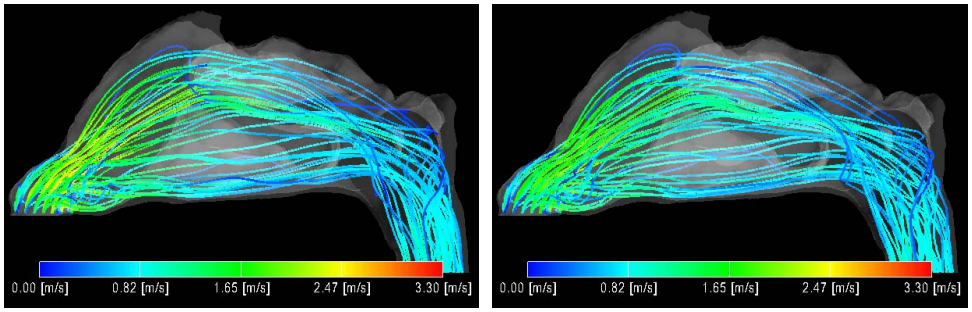

(a) Case A (b) Case B

Fig. 10 Flow in the Nasal Cavity:
Most air flowed through the middle and inferior meatuses. A small amount of air flowed through the superior meatus.

Figure 10 illustrates the flow in the nasal cavity by using streamlines. In both cases, the middle meatus, that is, the region between the inferior and middle nasal conchae, passed the maximum amount of air, and the flow velocity was high. The inferior meatus, that is, the region below the inferior nasal concha, passed the second-highest amount of air. The

superior meatus, that is, the region above the middle nasal concha, passed a small amount of air, and the flow velocity there was quite low. In case A, the air velocity in the nasal vestibule, that is, the region located immediately after the nares, was higher than that in case B, which was attributed to the total energy difference arising from the difference in the temperature of the inhaled air between cases A and B.

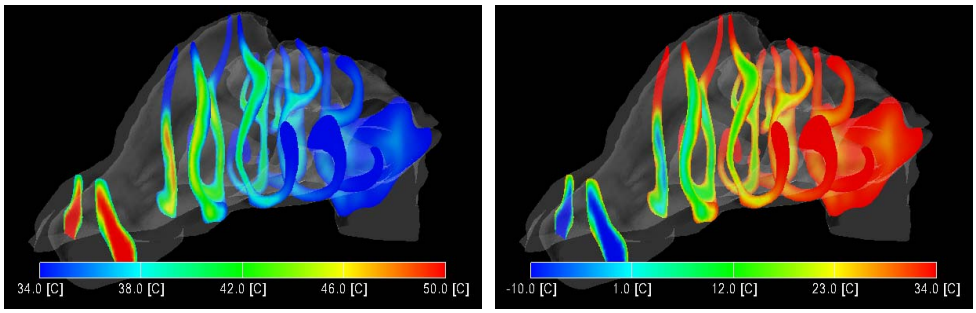

(a) Case A (b) Case B

Fig. 11 Temperature Distribution:
Temperature adjustment function of the nasal cavity works well in the front and narrow regions.

Figure 11 shows the temperature distribution in the nasal cavity by using contours. In case A, the air was cooled because it supplied heat to the organ side via the membrane. Figure 11(a) for case A indicates that the air temperature decreased with increasing distance from the nares. Most temperature change occurred in the front region of the nasal cavity. In addition, at a point located near the pharynx and at the narrow region of the nasal cavity, the hot inhaled air was sufficiently cooled to approximately the organ side temperature, 34 °C. In case B, the air became hot by absorbing heat from the organ side via the membrane. Figure 11(b) for case B indicates that the air temperature increased with increasing distance from the nares. Most temperature change also occurred in the front region of the nasal cavity. Furthermore, at a point located near the pharynx and at the narrow region of the nasal cavity, the cold inhaled air was sufficiently heated to approximately the organ side temperature, 34 °C.

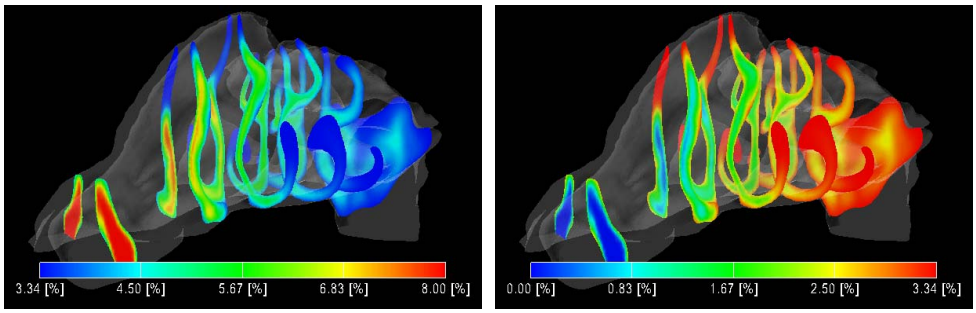

(a) Case A (b) Case B

Fig. 12 Mass Fraction of Water Distribution:
Humidity adjustment function of the nasal cavity works well in the front and narrow regions.

Figure 12 shows the mass fraction of water distribution in the nasal cavity by using contours. In case A, the air became dry because it supplied water into the organ side via the membrane. Figure 12(a) for case A indicates that the air became increasingly dry with increasing distance from the nares. Most of the change in the mass fraction of water occurred in the front region of the nasal cavity. Furthermore, at a point located near the pharynx and at the narrow region of the nasal cavity, the humid inhaled air was sufficiently

dried to approximately the organ side mass fraction of water, 3.34%. In case B, the air became humid by absorbing water from the organ side via the membrane. Figure 12(b) for case B indicates that the air became increasingly humid with increasing distance from the nares. Most of the change in the mass fraction of water also occurred in the front region of the nasal cavity. At a point located near the pharynx and at the narrow region of the nasal cavity, the dry inhaled air was sufficiently humidified to approximately the organ side mass fraction of water, 3.34%.

Figure 13(a) shows the temperature distribution for both cases. The horizontal and vertical axes represent the distance from the nares and the temperature, respectively. In case A, most temperature change occurred in the front region of the nasal cavity. The averaged temperature decreased to approximately the organ side temperature of 34 °C up to the pharynx. Similarly, in case B, the averaged temperature increased approximately to the organ side temperature of 34 °C. This change also occurred in the front region of the nasal cavity. Figure 13(b) shows the mass fraction of water distribution for both cases. The horizontal and vertical axes represent the distance from the nares and the mass fraction of water, respectively. In case A, similar to the temperature change, most of the changes in the mass fraction of water occurred in the front region of the nasal cavity. The averaged mass fraction of water decreased approximately to the organ side mass fraction of water, 3.34% up to the pharynx. In case B, the averaged mass fraction of water increased to approximately the organ side value of 3.34%. This change also occurred in the front region of the nasal cavity.

These results show that the temperature and humidity adjustment functions of the nasal cavity work efficiently in the front and narrow regions of the cavity.

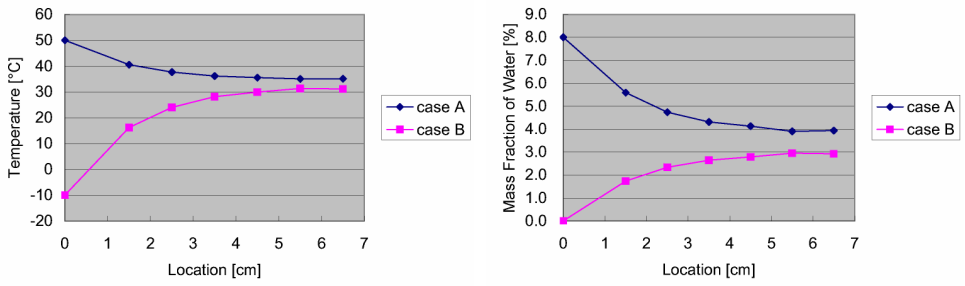

(a) Temperature (b) Mass Fraction of Water

Fig. 13 Temperature and Mass Fraction of Water Distribution:
Horizontal axis represents the distance form the nares. Temperature and mass fraction of water reached values that were approximately equal to the corresponding organ-side values.

6. Summary

To understand the temperature and humidity adjustment functions of the nasal cavity, heat and water exchange models were constructed for simulating the heat and water exchanges occurring on the nasal cavity wall. Because heat and water exchanges occur between the organ side and the air side via the mucous membrane in the nasal cavity, in our model, heat is transmitted between the organ side and the air side via the membrane by diffusion driven by a temperature difference. This model was incorporated into the computational fluid analysis as the boundary condition of the energy transport equation. Furthermore, water moves between the organ side and the air side via the membrane by diffusion driven by the water concentration difference, and this model was incorporated into the analysis as the boundary condition of the water transport equation by the double-film theory.

The simulation results obtained using the above models and a realistic nasal cavity shape reconstructed from CT images were compared with the measurements, and the reliability of these models was verified. Furthermore, by simulating two cases, hot-wet and cold-dry inhaled air, both air temperature and humidity were found to be described by values that were approximately equal to their respective organ side values. A significant change in the temperature and the mass fraction of water occurred in the front and narrow regions of the nasal cavity.

References

(1) Nishimura, T., Takai, M., Tsubamoto, T., Nakao, E. and Shigehara, N., Variation in maxilallry sinus anatomy among platyrrhire monkeys, Journal of Human Evolution, Vol.49 (2005), pp.370–389.

(2) Wen, J., Inthavong, K., Tu, J. and Wang, S., Numerical simulations for detailed airflow dynamics in a human nasal cavity, Respiratory Physiology & Neurobiology, Vol.161 (2008), pp.125–135.

(3) Finck. M., Hänel, D. and Wlokas, I., Simulation of nasal flow by lattice Bolzmann methods, Computers in Biology and Medicine, Vol.37 (2007), pp.739–749.

(4) Lee, J.H., Na, Y., Kim, S.K. and Chung, S.K., Unsteady flow characteristics through a human nasal cavity, Respiratory Physiology & Neurobiology, Vol.172 (2010), pp.136–146.

(5) Keck, T. and Leiacker, R., Humidity and temperature profile in the nasal cavity, Rhinology, Vol.38 (2000), pp.167–171.

(6) ANSYS, Inc. “ANSYS FLUENT Flow Modeling Software”. (online), available from <http://www.ansys.com/products/fluid-dynamics/fluent/>, (accessed 2010-10-12).

(7) Zachow, S., Muigg, P., Hildebrandt, T., Doleisch, H. and Hege, H.C., Visual exploration of nasal airflow, IEEE transactions on visualization and computer graphics, Vol.15, No.6 (2009), pp.1407–1414.

(8) Naftali, S., Rosenfeld, M., Wolf, M. and Elad, D., The Air-conditioning capacity of the human nose, Annals of Biomedical Engineering, Vol.33, No.4 (2005), pp.545–553.

(9) CYBERNET SYSTEMS CO., LTD. “DICOM 3D Viewer Real INTAGE (in Japanese),” (online), available from <http://kgt.cybernet.co.jp/feature/realintage01/>, (accessed 2010-10-12).

(10) Lorensen, W.E. and Cline, H.E., Marching Cubes: A high resolution 3D surface construction algorithm, Computer Graphics, Vol.21, No.4 (1987), pp.163–169.

(11) Nakayama, T., Ishikawa, S., Watanabe, M. and Matsuzawa, T., Simulation of airflow in nasal cavity for different breathing styles, Proc. The 6th International Conference on System Simulation and Scientific Computing (2005), pp.129–132.

(12) Materialize “Magics - Rapid Prototyping Software,” (online), available from <http://www.materialize.com/Magics>, (accessed 2010-10-12).

(13) Lee, C.Y. and Wilke, C.R., Measurements of vapor diffusion coefficient, Industrial and Engineering Chemistry, Vol.46, No.11 (1954), pp.2381–2387.